

Extrapolating statistics of turbulent flows to higher Re using quasi-steady theory of scale interaction in near-wall turbulence

Sergei I. Chernyshenko

Department of Aeronautics
Imperial College London
London SW7 2AZ, UK
s.chernyshenko@imperial.ac.uk

Chi Zhang

Department of Aeronautics
Imperial College London
London SW7 2AZ, UK
c.zhang13@imperial.ac.uk

Hamza Butt

Department of Aeronautics
Imperial College London
London SW7 2AZ, UK
hamza.butt15@imperial.ac.uk

Mohammad Beit-Sadi,

Department of Aeronautics
Imperial College London
London SW7 2AZ, UK
mohammad.beit-sadi13@imperial.ac.uk

ABSTRACT

A new technique for extrapolating statistical characteristics of near-wall turbulence from medium to higher Re is outlined. Results for extrapolating the velocity two-point correlation from $Re_\tau = 2003$ to $Re_\tau = 4179$ and for the parameters of an optimized comb probe for detecting the large-scale velocity component required for applying the technique in practice are presented.

MOTIVATION

Direct numerical simulations (DNS) and wind-tunnel experiments are typically done at the values of the Reynolds number Re below those characteristic for the practical applications. For the regions closest to the wall such results are usually extrapolated to higher Re on the basis of the classical universality hypothesis, according to which near the wall the turbulent flow parameters, expressed in the wall units, are independent of Re . However, the large-scale structures are not Re -independent, they grow as Re increases, and they affect the near-wall part of the flow (see the reviews by Marusic *et al.* (2010), Smits *et al.* (2011), and Jiménez (2012)). Hence, the classical universality hypothesis does not hold and there is a need for an alternative way of extrapolating turbulence statistics to higher Re .

BACKGROUND: QSQH THEORY

In the studies of scale interactions in near-wall turbulence, such as the pioneering study of Hutchins & Marusic (2007), the signals from the velocity probes are large-scale filtered, and the velocity is represented as a sum of large-scale and small-scale components, the relation between which is analyzed. The recent (Chernyshenko *et al.*, 2012; Zhang & Chernyshenko, 2016) quasi-steady quasi-homogeneous (QSQH) theory of scale interactions in near-wall turbulence is an alternative to the classic universality hypothesis. In essence, it amounts to defining the proper near-wall scaling of flow parameters similar to how it is done in the introduction of the well-known wall units, but with the friction velocity based on the large-scale-filtered friction instead of the friction velocity based on the time-averaged skin friction, and, accordingly, modifying the classical universality hypothesis by replacing the mean friction with the large-scale friction. The exact physical meaning of such a theory depends on the definition of large scale motions, which is a challenge. Zhang & Chernyshenko (2016) overcome it by postulating the specific properties of the large-scale filter. It is then up to the

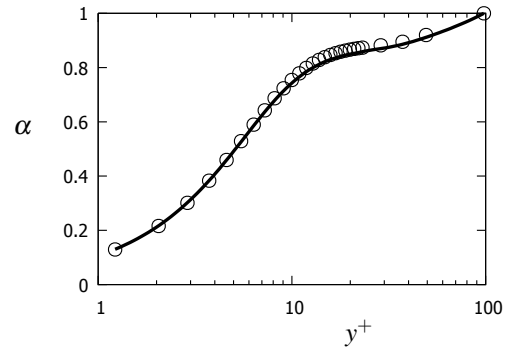


Figure 1. The superposition coefficient α introduced by Mathis *et al.* (2011), for $y_0^+ = 100$. The curve is the QSQH prediction (1), the symbols are DNS data by Agostini *et al.* (2014) at $Re_\tau = 1000$.

user to define a filter with properties as close as possible to these postulated properties. The benefit of such an approach is the possibility of doing rigorous mathematical derivations within the theory. This resulted in a number of nontrivial results, such as the explanation of the dependence of the mean-velocity log-law constants on Re consistent with the existence of the log-law itself, or relationships between parameters previously considered unrelated.

To verify the QSQH hypothesis, Zhang & Chernyshenko (2016) defined the large-scale filter as a Fourier cut-off filter, with cut-offs in time and two wall-parallel directions. The cut-off thresholds were selected using a multi-objective optimization, maximizing the two-point correlation between large scales and minimizing the two-point correlation between small scales directly at the wall and at a certain distance y_0 from the wall. The QSQH theory predicts that the well-known superposition coefficient $\alpha(y)$ introduced by Mathis *et al.* (2011) and the mean velocity profile $U(y)$ are related:

$$\alpha := \frac{\langle u'_L(y)u'_L(y_0) \rangle}{\langle u'^2_L(y_0) \rangle} \approx \frac{U(y) + ydU(y)/dy}{U(y_0) + y_0dU(y_0)/dy_0}, \quad (1)$$

where u'_L is the large-scale-filtered velocity fluctuation, y and y_0 are the wall-normal coordinates, and $\langle \cdot \rangle$ denotes averaging.

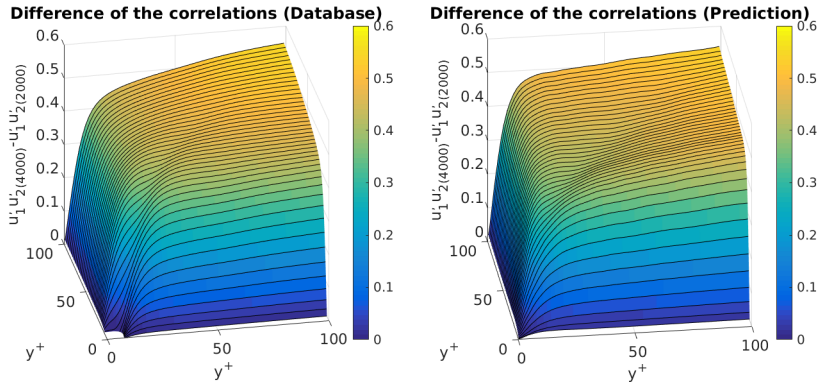


Figure 2. Actual (left) and extrapolated (right) distribution of $\langle u'(y_1)u'(y_2) \rangle|_{Re_\tau=4179} - \langle u'(y_1)u'(y_2) \rangle|_{Re_\tau=2003}$.

The agreement in figure 1 is particularly good. Within 100 wall units from the wall and at $Re_\tau = 1000$ the typical error of other QSQH predictions was found to be about 10%.

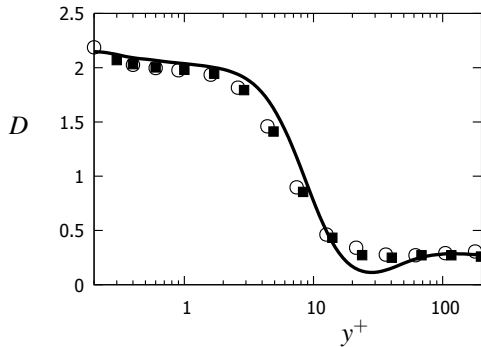


Figure 3. Curves are the QSQH prediction (2). Symbols are: \circ $Re_{\tau 1} = 1000, Re_{\tau 2} = 2003$; \blacksquare $Re_{\tau 1} = 2003, Re_{\tau 2} = 5186$. DNS data by Lee & Moser (2015)), $y_0^+ = 100$.

Equation (1) refers quantities at the same value of Re . As a first test of the possibility of applying the theory to extrapolation from one value of Re to another, Zhang & Chernyshenko (2016) compared the QSQH theory prediction relating the root-mean-square velocity $u_{rms}(y)$ at two values of Re to the mean velocity distribution:

$$D = y \frac{d}{dy} \ln \left(u_{rms}^2 \Big|_{Re_2} - u_{rms}^2 \Big|_{Re_1} \right) \approx y \frac{d}{dy} \ln \left(U(y) + y \frac{dU}{dy} \right)^2 \quad (2)$$

The comparison is shown in figure 3.

EXTRAPOLATION TECHNIQUE

To explain the extrapolation technique being proposed, more detail of the QSQH theory have to be explained. The QSQH theory introduces the large-scale-filtered skin friction τ_L and the corresponding friction velocity $u_{\tau_L}(t, x, z) = \sqrt{\tau_L(t, x, z)/\rho}$, where the variables have the commonly adopted meaning. A universal velocity function is then introduced such that

$$\tilde{u} \left(\frac{tu_{\tau_L}^2}{v}, \frac{xu_{\tau_L}}{v}, \frac{yu_{\tau_L}}{v}, \frac{zu_{\tau_L}}{v} \right) = \frac{u(t, x, y, z, Re)}{u_{\tau_L}(t, x, z, Re)}, \quad (3)$$

where all the quantities are total (not fluctuations), u is the flow velocity, and v is the kinematic viscosity. The QSQH theory postulates that near the wall at sufficiently high Re the statistical characteristics of $\tilde{u}(\tilde{t}, \tilde{x}, \tilde{y}, \tilde{z})$ for constant \tilde{t} , \tilde{x} , \tilde{y} , and \tilde{z} are independent of Re .

We propose the following 4-step procedure of extrapolating the turbulence statistics to Re so high that neither DNS nor near-wall experiments are feasible at the current state of the art.

- Step 1. An experiment or DNS is performed at a moderate $Re = Re_m$ to obtain $u(t, x, y, z, Re_m)$ and $u_{\tau_L}(t, x, z, Re_m)$.
- Step 2. The statistical properties of $\tilde{u}(\tilde{t}, \tilde{x}, \tilde{y}, \tilde{z})$ are determined from (3).
- Step 3. Measurements of $u_{\tau_L}(t, x, z, Re)$ are made at the high Re . This is easier than measuring $u(t, x, y, z, Re)$ because $u_{\tau_L}(t, x, z, Re)$ can be determined from measurements further away from the wall using the QSQH theory and because, being large-scale, it requires less spatial and temporal resolution.
- Step 4. The statistical properties of $u(t, x, y, z, Re)$ at the higher Re are obtained from (3).

To test this approach, we used the data for channel flow (Sillero & Jiménez, 2016) at $Re_\tau = 2003$ to predict the two-point velocity auto correlation function $\langle u'(y_1)u'(y_2) \rangle$ at $Re_\tau = 4179$. The comparison of the difference between the actual autocorrelation at $Re_\tau = 4179$ and $Re_\tau = 2003$ with the difference between the QSQH prediction for the autocorrelation at $Re_\tau = 4179$ and the actual autocorrelation at $Re_\tau = 2003$, shown in figure 2, is satisfactory.

IMPLEMENTATION

The existing DNS databases provide an implementation of Step 1, and experimental data can be used for this purpose as well. Step 2 is more complicated. A full statistical description of $\tilde{u}(\tilde{t}, \tilde{x}, \tilde{y}, \tilde{z})$ can be represented as a probability density distribution in a suitably-discretized functional space. This, however, is inefficient, because the dimension of the turbulent attractor is known to be far less than the dimension of the entire space, even if the latter is made finite by a suitable truncation, which is always the case in direct numerical simulations. The same problem is encountered in representing the statistical properties of the turbulent velocity field. This is overcome by storing a sufficiently long sample instance of a turbulent flow. In principle, the same solution can be used for $\tilde{u}(\tilde{t}, \tilde{x}, \tilde{y}, \tilde{z})$. The standard DNS database containing the values of the velocity at a discrete set in time and space can be converted into a database containing the values of \tilde{u} at a discrete set of $(\tilde{t}, \tilde{x}, \tilde{y}, \tilde{z})$ using (3). However, while the grid in the (t, x, y, z) space is usually regular, for example Cartesian, the corresponding grid in $(\tilde{t}, \tilde{x}, \tilde{y}, \tilde{z})$

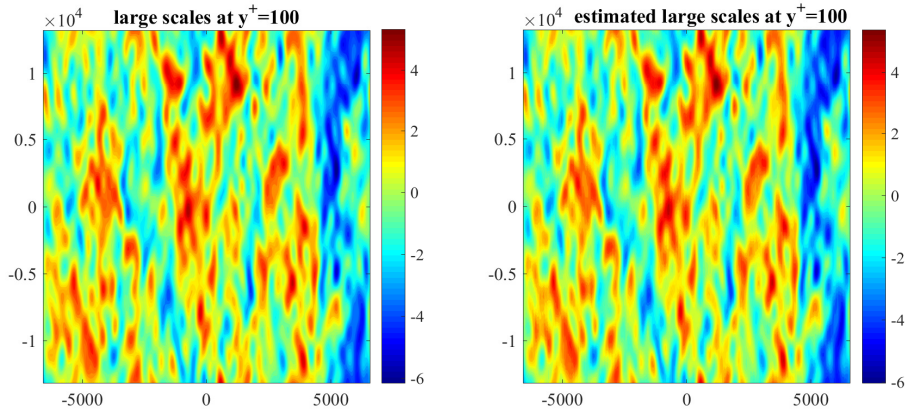


Figure 4. Actual (left) and obtained with the probe (right) large scales

space is not. Moreover, for large values of \tilde{t} , \tilde{x} , or \tilde{z} this grid self-overlaps. Zhang & Chernyshenko (2016) pointed out that in fact (3) is not applicable for large \tilde{t} , \tilde{x} , or \tilde{z} , and a more elaborate version of (3) should be used instead. This, however, makes creating the $\tilde{u}(\tilde{t}, \tilde{x}, \tilde{y}, \tilde{z})$ cumbersome. Instead, the database for $Re = Re_m$ together with the corresponding $u_{\tau_L}(t, x, z, Re_m)$ can be used for recalculating \tilde{u} from (3) every time it is needed.

The difficulty of implementing Step 3 depends on the definition of the large-scale filter. For example, implementing the Fourier cut-off filter used in (Zhang & Chernyshenko, 2016) requires at the least the knowledge of the time series of noticeably greater length than the time cut-off, and in a domain of the longitudinal and spanwise dimensions also much greater than the corresponding cut off lengths. Such knowledge can be obtained by DNS. For example, for making the extrapolation of the two-point auto-correlation shown in figure 2 we obtained $u_{\tau_L}(t, x, z, Re_\tau)$ at $Re_\tau = 4179$ from the DNS database for $Re_\tau = 4179$. In a practical application this would not be possible, since, having that much data at the target value of Re_τ , one would not need to extrapolate.

To resolve this difficulty, we propose to use in experiments several probes arranged in a rake pattern in the spanwise direction. The probes can be located at a certain distance y_0 of about 100 wall units from the wall since, according to the QSQH results already verified (Zhang & Chernyshenko, 2016), the large-scale motion is well correlated in wall normal direction up to this distance, and the further away from the wall the probes are located the easier it is to make the measurements. The probes will measure the velocity, and the large-scale friction will then be obtained with the help of the QSQH theory. The approximation $u_{L,p}(t, x, y_0, z)$ for the actual $u_L(t, x, y_0, z)$ can then be obtained as

$$u_{L,p}(t, x, y_0, z) = \sum_{k=1}^n w_k u(t, x, y_0, z + \Delta z_k), \quad (4)$$

where Δz_k is the spanwise displacement of the k -th probe within the rake, and n is the number of the probes. The weights w_k and the displacements Δz_k between the probes should be optimized to minimize the difference between $u_{L,p}$ and the actual u_L .

THE 9-PROBE RAKE FOR $Re_\tau = 4179$ DATABASE

We will now describe the preliminary calculation of the optimal probe for the case when the database used as the basis for extrapolation is the plane channel flow database for $Re_\tau = 4179$

(Sillero & Jiménez, 2016), and the large-scale motions are defined by a spatial Fourier cut-off filter with the cut-off lengths $L_x^+ = 3282$ and $L_z^+ = 386.1$, which are the values accepted in (Zhang & Chernyshenko, 2016). Note that in (Zhang & Chernyshenko, 2016) the filter also used a cut-off in time, and it was optimized for $Re_\tau = 1000$. Abandoning the time cut-off is justified by the approximate validity of the Taylor hypothesis in this context. In experiment using a cut-off in x will not be possible, and, hence, using the cut-off in x as a proxy for cut-off in time is the best option in optimizing the probe. However, ideally, the cut-off values should be selected to correspond to Re_τ of the database to be used for optimization. This is yet to be done in the future work.

We have selected one time frame from the database, and concentrated on a particular grid layer at the distance $y_0^+ = 99$, obtaining a slice of the velocity in the form $u = u(x_i, z_j)$, where x_i and z_j are the grid line coordinates. We then applied to this slice the Fourier cut-off filter described above and obtained the corresponding large-scale component $u_L(x_i, z_j)$. The number of probes n was assumed to be equal to 9, equal to the number of available signal processing channels in a specific possible future experimental implementation. Selecting a particular set of probe displacements Δz_k , the optimal weights can be found by minimizing the L_2 norm of the difference between u_L and $u_{L,p}$, which is equivalent to the following easily solvable quadratic optimization problem

$$\min_{\Delta z_k} \sum_{i,j} (u_L(x_i, z_j) - u_{L,p}(x_i, z_j))^2$$

with $u_{L,p}$ defined by (4). We then used two approaches for optimizing Δz_k . In one approach the probes were assumed to be evenly spaced, $\Delta z_k = (k-5)\Delta z$. Optimization with respect to a single parameter Δz is then fast and straightforward. In the second approach the set of Δz_k values was optimized using the genetic optimization algorithm included in MATLAB. In all cases we assumed the probe spacing to be symmetric with respect to the center probe. On obtaining the weights we inspected their symmetry as a way of verification, since if the probes are symmetric the weights should also be symmetric. The large-scale field obtained with the optimal genetically-optimized probe is compared with the actual large-scale field in figure 4. We defined the relative error as $\|u'_L - u'_{L,p}\| / \|u'_L\|$, where prime denotes the fluctuation. For the same slice that the probe was optimized, the genetically optimized rake gave the error of 0.0715 and the evenly spaced probe gave the error of 0.0826. For

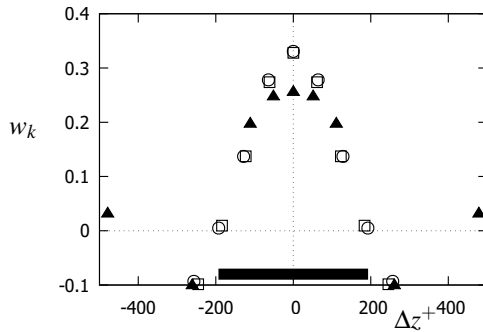


Figure 5. Weights: \circ uniform $Re_\tau = 4178$, \square uniform $Re_\tau = 2003$, \blacktriangle genetically optimized $Re_\tau = 4178$. The horizontal bar shows the cut-off length.

a different time step, the same weights gave the errors 0.0779 and 0.0905 respectively.

The probe positions and weight of the genetically optimized rake are shown in Table 1. For a uniformly-spaced probes the probe spacing was found to be $\Delta z^+ = 64.13$, while the weights were 0.3306, 0.2783, 0.1369, 0.0050, -0.0932 , starting from the center probe. Due to symmetry, the values for only one side of the rake are provided here and in the table.

Table 1. Optimal probe displacement and weights.

Δz_k^+	w_k
0	0.2564
51.3	0.2482
111.6	0.1979
260.8	-0.0999
478.8	0.0322

Figure 5 shows these weights and probe positions together with the weights and positions of the optimal uniformly-spaced weights probe for the database for $Re_\tau = 2003$. It can be observed that the Reynolds number has little effect on the optimal probe, and that the main effect of the genetic optimization amounts to moving the probe that has almost zero weight in the uniformly-spaced probe to a new position.

Finally, figure 6 shows the gain of the probe filter as compared with the gain of the cut-off filter, and a suitably-scaled premultiplied velocity spectrum. It can be seen that the optimization procedure trades off the agreement of the gains at the wavenumbers with low

energy for the better agreement of the gain at the higher energy, as it can indeed be expected.

It can be concluded that a systematic procedure of extrapolation of turbulent statistics of near wall flow, taking into account the effect of large-scale structures, has been developed. It remains yet to be implemented in practice.

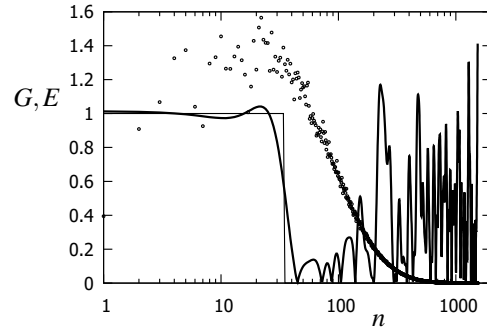


Figure 6. Filter gains G and premultiplied spectrum E versus the wavenumber n . Straight lines show the gain of the Fourier cut-off filter, the curve is the gain of the genetically-optimized 9-probe filter, and symbols are a sample of a premultiplied velocity spectrum.

REFERENCES

- Agostini, L., Toubert, E. & Leschziner, M. A. 2014 Spanwise oscillatory wall motion in channel flow: Drag-reduction mechanisms inferred from DNS-predicted phase-wise property variations at $Re_\tau=1000$. *J. Fluid Mech.* **743**, 606–635.
- Chernyshenko, S., Marusic, I. & Mathis, R. 2012 Quasi-steady description of modulation effects in wall turbulence. *arXiv:1203.3714 [physics.flu-dyn]*.
- Hutchins, N. & Marusic, I. 2007 Large-scale influences in near-wall turbulence. *Phil. Trans. Roy. Soc.* **365** (1852), 647–664.
- Jiménez, J. 2012 Cascades in wall-bounded turbulence. *Ann. Rev. Fluid Mech.* **44** (1), 27–45.
- Lee, M. & Moser, R. D. 2015 Direct numerical simulation of turbulent channel flow up to $Re_\tau=5200$. *J. Fluid Mech.* **774**, 395–415.
- Marusic, I., McKeon, B. J., Monkewitz, P. A., Nagib, H. M., Smits, A. J. & Sreenivasan, K. R. 2010 Wall-bounded turbulent flows at high Reynolds numbers: Recent advances and key issues. *Phys. Fluids* **22** (6).
- Mathis, R., Hutchins, N. & Marusic, I. 2011 A predictive inner-outer model for streamwise turbulence statistics in wall-bounded flows. *J. Fluid Mech.* **681**, 537–566.
- Sillero, J. A. & Jiménez, J. 2016 Editorial opinion: public dissemination of raw turbulence data. *J. Physics: Conf. Ser.* **708**, 011002.
- Smits, A. J., McKeon, B. J. & Marusic, I. 2011 High Reynolds number wall turbulence. *Ann. Rev. Fluid Mech.* **43** (1), 353–375.
- Zhang, C. & Chernyshenko, S.I. 2016 Quasisteady quasihomogeneous description of the scale interactions in near-wall turbulence. *Phys. Rev. Fluids* **1**, 014401.